Research Article

MOLECULAR PAIN

Upregulation of KDM6B in the anterior cingulate cortex contributes to neonatal maternal deprivation-induced chronic visceral pain in mice

Molecular Pain
Volume 20: 1–14
© The Author(s) 2024
Article reuse guidelines:
sagepub.com/journals-permissions
DOI: 10.1177/17448069241260349
journals.sagepub.com/home/mpx
Sage

Zi-Long Yi[1], Jin-Nan Lu[1], Jin-Jin Zhu[1], Tian-Tian He[1], Yi-Ran Xu[1], Zi-Wei Huang[1], Yong-Chang Li[2], and Guang-Yin Xu[1,2]

Abstract

Irritable bowel syndrome (IBS) is a prevalent functional gastrointestinal disease characterized by chronic visceral pain with a complex etiology and challenging treatment. Although accumulating evidence supports the involvement of central nervous system sensitization in the development of visceral pain, the precise molecular mechanisms remain incompletely understood. In this study, we highlight the critical regulatory role of lysine-specific demethylase 6B (KDM6B) in the anterior cingulate cortex (ACC) in chronic visceral pain. To simulate clinical IBS conditions, we utilized the neonatal maternal deprivation (NMD) mouse model. Our results demonstrated that NMD induced chronic visceral pain and anxiety-like behaviors in mice. Notably, the protein expression level of KDM6B significantly increased in the ACC of NMD mice, leading to a reduction in the expression level of H3K27me3. Immunofluorescence staining revealed that KDM6B primarily co-localizes with neurons in the ACC, with minimal presence in microglia and astrocytes. Injecting GSK-J4 (a KDM6B-specific inhibitor) into ACC of NMD mice, resulted in a significant alleviation in chronic visceral pain and anxiety-like behaviors, as well as a remarkable reduction in NR2B expression level. ChIP assay further indicated that KDM6B regulates NR2B expression by influencing the demethylation of H3K27me3. In summary, our findings underscore the critical role of KDM6B in regulating chronic visceral pain and anxiety-like behaviors in NMD mice. These insights provide a basis for further understanding the molecular pathways involved in IBS and may pave the way for targeted therapeutic interventions.

Keywords

Irritable bowel syndrome, chronic visceral pain, KDM6b, anterior cingulate cortex, NR2b

Date Received: 9 March 2024; Revised 18 April 2024; accepted: 19 May 2024

Introduction

Irritable bowel syndrome (IBS) is a prevalent gastrointestinal disorder characterized by chronic visceral pain, typically presenting as abdominal discomfort or pain along with altered bowel habits.[1–3] Globally, IBS affects approximately 11 % of the population,[4–6] with direct economic costs exceeding $ 1 billion in the United States.[7,8] The pathogenesis of IBS centers around abnormalities in visceral sensation, neurologic processing of pain, gut-brain interactions, and psychosocial distress.[9–11] Despite extensive research, the exact molecular mechanisms remain incompletely elucidated.[12] Previous

[1]Henan Key Laboratory of Child Brain Injury and Henan Pediatric Clinical Research Center, The Third Affiliated Hospital and Institute of Neuroscience of Zhengzhou University, Zhengzhou, China
[2]Jiangsu Key Laboratory of Neuropsychiatric Diseases and Institute of Neuroscience, Soochow University, Suzhou, China

Corresponding Authors:
Guang-Yin Xu, Center for Translational Pain Medicine, Institute of Neuroscience, Soochow University, 199 Renai Rd, Suzhou 215123, China.
Email: guangyinxu@suda.edu.cn

Yong-Chang Li, Center for Translational Pain Medicine, Institute of Neuroscience, Soochow University, 199 Renai Rd, Suzhou 215123, China.
Email: yongchangli@suda.edu.cn

Creative Commons Non Commercial CC BY-NC: This article is distributed under the terms of the Creative Commons Attribution-NonCommercial 4.0 License (https://creativecommons.org/licenses/by-nc/4.0/) which permits non-commercial use, reproduction and distribution of the work without further permission provided the original work is attributed as specified on the SAGE and Open Access pages (https://us.sagepub.com/en-us/nam/open-access-at-sage).

studies have shown that chronic visceral pain in IBS patients may stem from psychological abnormalities linked to adverse childhood experiences.[10,13] To further explore this, neonatal maternal deprivation (NMD) serves as a well-established early life stress model, inducing chronic visceral pain in adult mice.[14,15]

The anterior cingulate cortex (ACC), situated in the anterior part of the cerebral cortex above the corpus callosum, plays a pivotal role in emotion, attention, memory, and pain processing.[16–18] Recent studies have indicated its association with comorbidities of pain and mood disorders, including anxiety and depression.[16,19–24] Increasing evidence suggests that ACC is intimately associated with chronic visceral pain caused by IBS. In multiple animal models of chronic visceral pain, the ACC show dramatically activation.[25–29] The ACC contributes to the development of chronic visceral pain by regulating the function of diverse molecules and neural circuits.[14,30–34]

In recent years, the role of epigenetics in pain development has been confirmed, with particular significance in chronic visceral hypersensitivity.[35,36] Study have emphasized that epigenetics is a crucial mechanism underlying the generation of chronic visceral hypersensitivity.[37] Previous studies have revealed altered levels of histone methylation, histone acetylation, and DNA methylation in models of chronic stress-induced visceral pain,[38–42] further suggesting the importance of epigenetics in visceral hypersensitivity. Lysine-specific demethylase 6B (KDM6B, also known as JMJD3) plays a specific role in demethylating trimethylated lysine 27 (H3K27me3) of histone H3, resulting in the upregulation of gene expression.[43] KDM6B is involved in critical cellular processes such as cell differentiation, development, tumorigenesis, inflammatory diseases, and neurodegenerative disorders.[44,45] Despite its known roles, the contribution of KDM6B to chronic visceral pain has remained unclear. Recent studies have shown that KDM6B-mediated demethylation of H3K27me3 contributes to the promotion of chronic postsurgical pain (CPSP).[46] Notably, the inhibitor of KDM6B, GSK-J4, has shown significant attenuation of neuropathic pain in rats,[47–49] evidencing that KDM6B plays a critical role in the development and maintenance of neuropathic pain. This compelling evidence leads us to speculate that KDM6B may play a crucial regulatory role in the development of chronic visceral pain.

In this study, we present compelling evidence demonstrating that KDM6B regulates NR2B expression by modulating the demethylation of H3K27me3, thereby exerting a regulatory effect on chronic visceral pain. This insight opens new avenues for the treatment of chronic visceral pain, potentially contributing to the development of novel analgesic drugs and therapeutics.

Materials and methods

Animals

Adult male and female C57BL/6 mice were used for breed. The mice were purchased from Beijing Vital River Laboratory Animal Technology Co., Ltd. After delivery, the male pups were selected for induction of chronic visceral pain. All mice used in the experiments were housed one to five mice per cage depending on the experimental requirements. The animals were provided with free access to standard mouse feed and water and were kept under a 12 h light/dark cycle at a constant temperature of 23°C–25°C. All experimental procedures were approved by The Third Affiliated Hospital of Zhengzhou University and adhered to the guidelines of the International Association for the Study of Pain.

Chronic visceral pain model

Chronic visceral pain was caused by neonatal maternal deprivation (NMD), as previously reported.[50,51] Briefly, 1 day after birth (P1), mice were placed in a special isolation box for neonatal maternal deprivation. Each pup occupied a small compartment in the isolation box.[52] The temperature and humidity of the isolation box were kept consistent with the feeding environment, and the bottom was covered with soft cotton to protect the mice from harm. Modeling started at P1 and ended at P14 with 3 h of maternal deprivation daily.[14] The control group received no treatment.

Colorectal distention threshold

Colorectal distention (CRD) is a well-established method for measuring visceral pain threshold.[53] During the procedure, mice were fully anesthetized with isoflurane. A special 1.5 cm flexible balloon was then inserted 2 cm into the anus and secured to the tail with pressure-sensitive tape to prevent slipping. The mice were placed in a customized transparent resin box (15 × 3.5 × 4 cm) and allowed to wake up and adapt for 30 min. Gas was slowly injected into the balloon via a sphygmomanometer until the mice exhibited visceral pain behaviors such as abdominal contractions or head raising. At this point, the gas injection was stopped and the sphygmomanometer reading was recorded. Measurements were repeated five times per mouse, with each measurement separated by 3 min to avoid tissue damage. The average of the five measurements was used to determine the colorectal distention threshold of the mice. All behaviors experiments were performed in a double-blinded trials.

Open field test

Open field test (OFT, 45 × 45 × 45 cm, Global Biotech, China) was employed to assess motor function and anxiety-like behaviors. All mice were adapted to the experiment environment for 3 h before the OFT. Each mouse was placed in the center of the OFT apparatus. The center zone was defined as a square, 10 cm away from the wall. This study used the animal behaviors analysis software (ANY-maze, Stoelting, USA) to record 5 min of data for each mouse in

this test. The behaviors experiments were conducted as double-blinded trials.

Elevated zero maze

Elevated zero maze (EZM, Global Biotech, China) was performed to test anxiety-like behaviors, which comprises a circular track with a diameter of 50 cm and a width of 5 cm, divided into two open areas and two closed areas by four partitions. All mice were adapted to the experiment environment for 3 h before the test. Each mouse was placed in the open area of the EZM apparatus. This study used the animal behaviors analysis software (ANY-maze, Stoelting, USA) to record 3 min of data for each mouse in this test. All behaviors experiments were conducted as double-blinded trials.

Rotarod test

The rotarod test (Global Biotech, China) was utilized to evaluate the motor function of mice. Before the test, the mice were allowed to acclimatize to the experimental environment for 3 h. They were placed on a constantly accelerating (5∼40 r/min) rotor for 3 min and the dwell time was recorded. The experiment was repeated 3 times for each mouse, with a 30 min rest between each repetition. All behaviors experiments were conducted as double-blinded trials.

Western blotting

The anterior cingulate cortex (ACC), prefrontal cortex (PFC), and insular cortex (IC) were isolated after the brain tissue was stripped and rapidly transferred then to liquid nitrogen. Next, the samples were homogenized with ice-cold RIPA lysis buffer (Yeasen, China), protease inhibitor (Selleck, USA), and phosphatase inhibitor (Selleck, USA). The crude homogenate was centrifuged at 4°C for 30 min at 12000 r/min/min, and the supernatants were collected. The protein concentration was measured using the BCA method, and the sample was heated at 95°C for 10 min. The protein samples were electrophoresed using 4 %-20 % gradient polyacrylamide gels (Yeasen, China) at 120 V. Subsequently, the proteins were transferred to PVDF membranes (Millipore, USA). The blotting membranes were blocked with 5 % nonfat milk at room temperature for 1 h and then incubated with the primary antibody overnight at 4°C. On the following day, the membranes were incubated with the secondary antibody at room temperature for 2 h. The proteins on the blotting membranes were visualized using the ECL Chemiluminescence Kit (Epizyme, China). The gray value of the western blot was quantified using Image Lab (Bio-Rad, USA). Primary antibodies of anti-GAPDH (1:1000, rabbit, Cell Signaling Technology, USA), anti-KDM6B (1:1000, rabbit, Abcam, UK), anti-H3K27me3 (1:1000, mouse, Abcam, UK), anti-H3 (1:1000, rabbit, Abcam, UK) were used. Secondary antibodies of goat anti-rabbit IgG H&L HRP (1:10000, Abcam, UK), goat anti-mouse IgG H&L HRP (1:10000, Thermo Fisher Scientific, USA) were used.

Table 1. Primer sequences used in qPCR

Gene	Primers	Sequences (5'-3')
KDM6B	Forward	TGAAGAACGTCAAGTCCATTGTG
	Reverse	TCCCGCTGTACCTGACAGT
NR2B	Forward	GCCATGAACGAGACTGACCC
	Reverse	GCTTCCTGGTCCGTGTCATC
GAPDH	Forward	AGGTCGGTGTGAACGGATTTG
	Reverse	TGTAGACCATGTAGTTGAGGTCA

Real-time quantitative PCR (qPCR)

The total RNA in the tissue was extracted according to the protocol of the RNAsimple Total RNA Kit (TIANGEN, China). RNA sample of the ACC was reversely transcribed to cDNA using the T100 Thermal Cycler PCR instrument (Bio-Rad, USA) according to the cDNA Synthesis kit (Yeasen, China). Then, the mRNA expressions of genes were detected by LightCycler 96 (Roche, Switzerland). The data of qPCR were analyzed using the ΔΔCt method. Tables 1 and 2

Immunofluorescence

Mice were perfused transcardially with 0.9 % saline and 4 % paraformaldehyde (Biosharp, China), and post-fixed in 4 % paraformaldehyde for 2 h. Next, brain tissues were dehydrated by sucrose solution at a concentration gradient of 10–30 % followed by embedding using Tissue-Tek O.C.T. Compound (Sakura, USA). The brains of the mice were sliced into 20 μm sections using a freezing microtome (Leica, Germany). After the brain sections were repaired with sodium citrate at 95°C for 30 min, they were blocked with 10 % goat serum and 0.3 % Triton X-100 at room temperature for 1 h. Subsequently, the sections were incubated with the primary antibody at 4°C overnight. The next day, the brain slices were cleaned with PBS for 3 times and incubated with the secondary antibody at room temperature for 1 h. Immunofluorescence images for cell statistics were captured using a scanning machine (KFBIO, China), while immunofluorescence images for display were captured using the laser confocal microscopy (LSM 900, ZEISS, Germany). Cell counting was performed using HALO software (Indica Labs, USA). Primary antibodies of anti-KDM6B (1:200, rabbit, ABclonal, China), anti-GFAP (1:500, guinea pig, Oasis Biofarm, China), anti-NeuN (1:500, mouse, Oasis Biofarm, China), anti-Iba1 (1:500, mouse, Oasis Biofarm, China) were used. Secondary antibodies of goat anti-guinea pig Alexa Fluor 647 (1:500, Oasis Biofarm, China), goat anti-mouse Alexa Fluor 488 (1:500, Thermo Fisher Scientific, USA), goat anti-rabbit Alexa Fluor 555 (1:500, Thermo Fisher Scientific, USA) were used.

Table 2. Primer sequences used in ChIP-qPCR.

Gene	No.	Primers	Sequences (5'-3')
NR2B promoter	P1	Forward	CATAACGCAGATGGCTCAGG
		Reverse	TCTCGTGCGTAGATCATCCC
	P2	Forward	GCGCAACCTCACTTTGTCTC
		Reverse	ACGACACACAGAGGAGAACAC
	P3	Forward	TTCCTGGTGCTGACTGGACTA
		Reverse	ATGGCAGTAAAACAACGGGC
	P4	Forward	AGGGGAGTGGTTTCAGTGTC
		Reverse	TGGCAGCAAGAAGGAATAGCA

Drug application

DMSO (1 μl) and GSK-J4 (0.005 mg/kg, 0.025 mg/kg, 0.1 mg/kg, 1 μl) were injected into the right ACC (AP: +1.0 mm, ML: +0.3 mm, DV: −2.5 mm) using stereotaxic. The animals were deeply anesthetized with 1 % pentobarbital and firmly fixed to the brain stereotaxic apparatus (REWARD, China) to ensure that the entire skull plane was horizontal. The skin of the mouse's head was cut to fully expose the skull. To align the needle pair of the microinjector with the location of the bregma point of the mouse, set this point as the origin using the software. Then, entering the coordinates of the ACC into the software to move the needle to ACC region. Subsequently, using the skull drill to make a small 1 mm diameter hole in this position. The injection begins at 500 nL/min as the needle enters the ACC through the hole. After completing the injection, the syringe was left undisturbed for 5 min.

Chromatin immunoprecipitation (ChIP)-qPCR assay

ChIP-qPCR assay was conducted using a ChIP Kit (Thermo Fisher Scientific, USA) and followed its protocol. In brief, ACC was crosslinked with 1 % paraformaldehyde for 15 min at room temperature, which was terminated by adding 10 % glycine. DNA within ACC was then digested into 150 bp-1000 bp fragments using lysate buffer and micrococcal nuclease (MNase). H3K27me3 and IgG antibodies were added to the DNA fragments and incubated at 4°C overnight. Subsequently, DNA fragments bound by antibodies were enriched using magnetic beads. The enriched DNA was then eluted and used as the sample for subsequent PCR and qPCR experiments.

Data analysis

All data were presented with mean ± sem, and normality was checked for all data before comparison. GraphPad Prism 9 (GraphPad Software, USA) was used for statistical analysis and for revising statistical graphs. This study employed several statistical tests, including two sample *t* test, Mann Whitney test, two-way ANOVA followed by Bonferroni's test. Statistical significance was determined at $p < .05$.

Results

NMD induced chronic visceral pain and anxiety-like behaviors

The timeline of NMD modeling was shown in Figure 1(a). Chronic visceral pain was evaluated by CRD and found that NMD mice exhibit chronic visceral pain at 6w-10w (Figure 1(b), $n = 10$, $^{***}p < .001$, two-way ANOVA followed by Bonferroni's test). Consistent with previous studies, NMD successfully induced chronic visceral pain in mice.[33,54] Subsequently, the open field test, the elevated zero maze, and the rotarod test were performed to assess anxiety-like behaviors. During the open field test, NMD mice spent less time in the center zone and more time exploring the corner zone (Figure 1(c)–(e), n = 18-20, $^{*}p < .05$, $^{**}p < .01$, two sample *t* test) compared with CON mice. However, there was no significant difference in the number of times the two groups of mice entered the center zone (Figure 1(f), n = 18-20, two sample *t* test). Although there was no significant difference in the total distance between the two groups, NMD mice were found to be more active in the open field than CON mice (Figure 1(g) and (h), n = 18-20, $^{**}p < .01$, two sample *t* test). The results of the elevated zero maze showed that NMD mice spent less time exploring open zone than CON mice (Figure 1(i) and (j), n = 18-20, $^{*}p < .05$, two sample *t* test). There was no difference in the distance traveled in the open zone or the number of times entered the open zone (Figure 1(k) and (l), n = 18-20, two sample *t* test). The rotarod test indicated that there was no significant difference in motor function between the two groups of mice (Figure 1(m), $n = 6$, two sample *t* test). These findings suggest that NMD mice exhibited persistent and stable chronic visceral pain with anxiety-like behaviors that did not affect motor function.

KDM6B expression was upregulated in the ACC of NMD mice, whereas H3K27me3 expression was decreased

KDM6B mRNA expression in the ACC of NMD mice was significantly increased compared with CON mice by qPCR assay (Figure 2(a), $n = 5$, $^{**}p < .01$, Mann Whitney test). Western blotting was performed to detect KDM6B and H3K27me3 protein level in ACC of 6-week-old NMD mice and

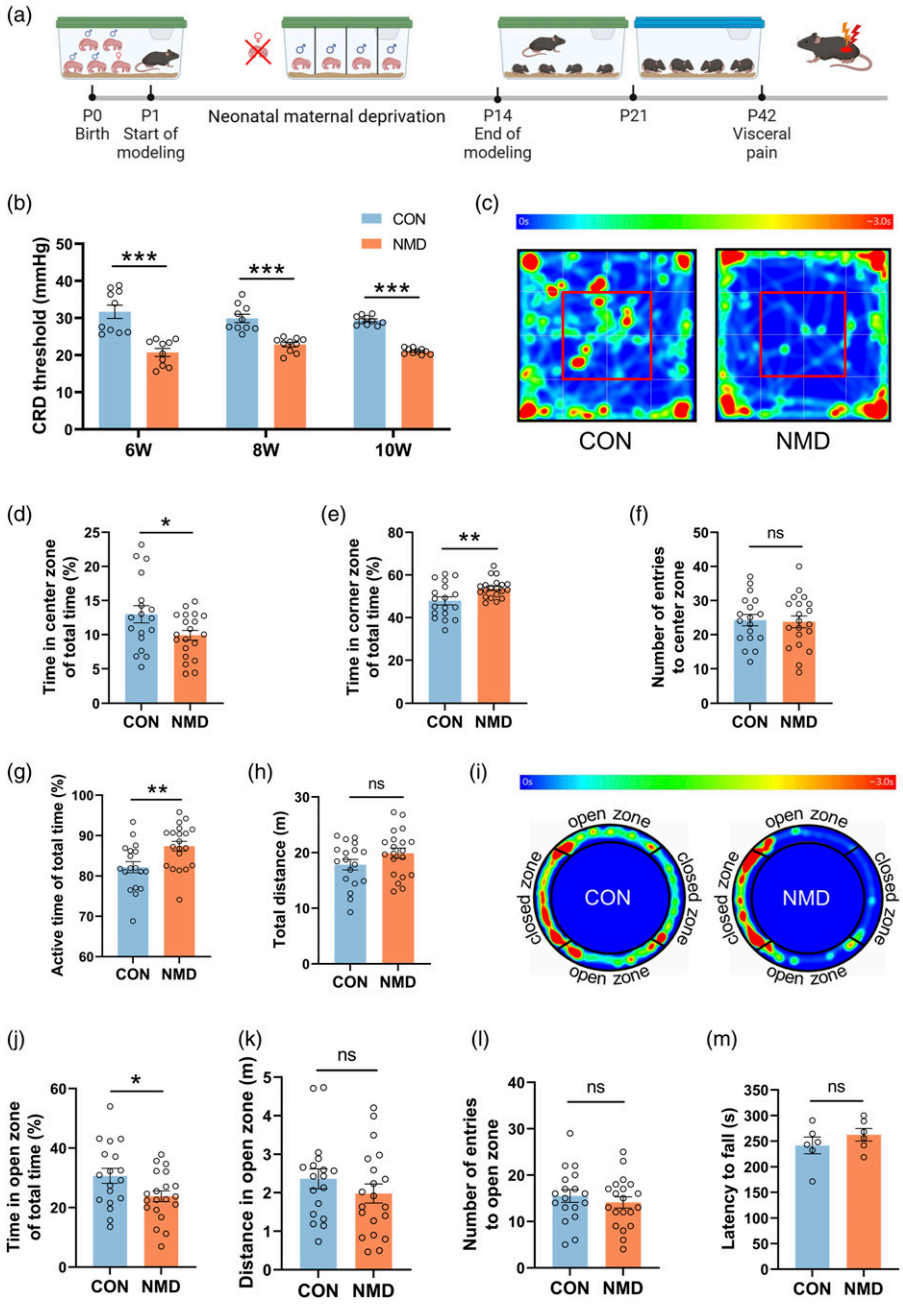

Figure 1. NMD induced chronic visceral pain and anxiety-like behaviors in mice. (a) Timeline of NMD modeling process. (b) CRD threshold of CON and NMD mice at 6-10 weeks of age. (n = 10, ***p < .001, two-way ANOVA followed by Bonferroni's test). (c) Heat maps of CON and NMD mice in the 5 min open field tests were detected by ANY-maze (the red square represents the center zone). (d)-(h) Analysis of time in center zone of total time (d), time in corner zone of total time (e), number of entries to center zone (f), active time of total time (g), total distance (h) of CON and NMD mice in the open field test (n = 18-20, *p < .05, **p < .01, two sample t test). (i) Heat maps of CON and NMD mice in the 3 min elevated zero maze tests were detected by ANY-maze. (j-l) Analysis of time in open zone of total time (j), distance in open zone (k), number of entries to open zone (l) of CON and NMD mice in the elevated zero maze test (n = 18-20, *p < .05, two sample t test). (m) Analysis of latency to fall of CON and NMD mice in the rotarod test (n = 6, two sample t test).

CON mice. The statistical results indicated that the protein level of KDM6B was significantly upregulated in the ACC of NMD mice compared to CON mice (Figure 2(b) and (c), n = 6, ***p < .001, two sample t test), while the corresponding protein expression of H3K27me3 was significantly decreased (Figure 2(b) and (d), n = 6, **p < .01, two sample t test). Importantly, to assess the specificity of the upregulation of KDM6B and H3K27me3 expression in the ACC region, we performed the same operation in the PFC and IC regions. There was no significant difference in the PFC (Figure 2(e)–(g), n = 6, two

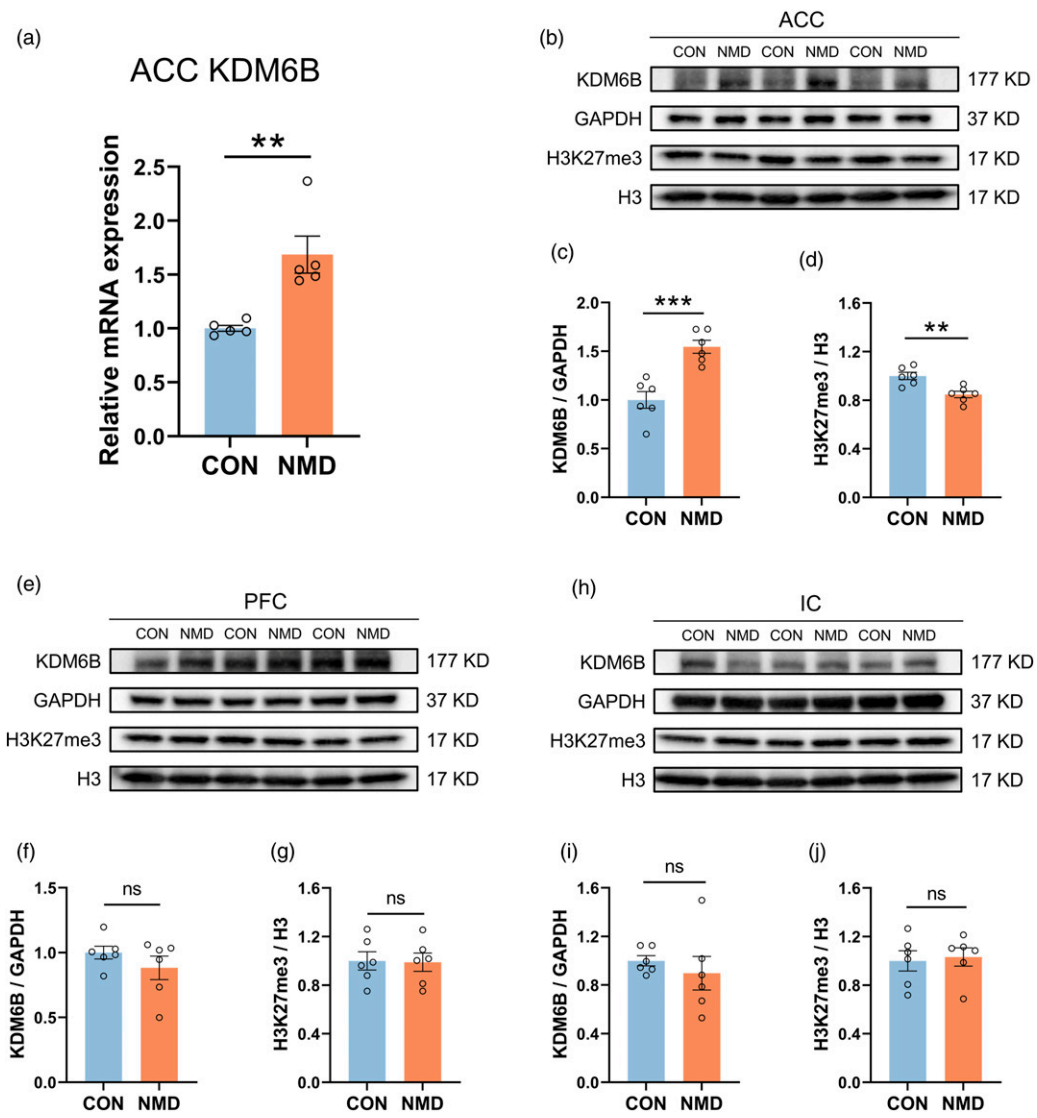

Figure 2. NMD induced upregulation of KDM6B and downregulation of H3K27me3 in the ACC of mice. (a) Quantification of KDM6B mRNA expression in the ACC of CON and NMD mice (n = 5, $^{**}p < .01$, Mann Whitney test). (b) Representative western blotting of KDM6B, GAPDH, H3K27me3, and H3 in the ACC of CON and NMD mice. (c)-(d) Quantification of KDM6B (c) and H3K27me3 (d) expression in the ACC of CON and NMD mice (n = 6, $^{**}p < .01$, $^{***}p < .001$, two sample t test). (e) Representative western blotting of KDM6B, GAPDH, H3K27me3, and H3 in PFC of CON and NMD mice. (f)-(g) Quantification of KDM6B (f) and H3K27me3 (g) expression in PFC of CON and NMD mice (n = 6, two sample t test). (h) Representative western blotting of KDM6B, GAPDH, H3K27me3, and H3 in IC of CON and NMD mice. (i)-(j) Quantification of KDM6B (i) and H3K27me3 (j) expression in IC of CON and NMD mice (n = 6, two sample t test).

sample t test) and IC (Figure 2(h)–(j), n = 6, two sample t test). These findings show that protein levels and mRNA expression of KDM6B were significantly upregulated in the ACC of NMD mice but did not affect expression in the IC and PFC regions, suggesting that the increased expression of KDM6B in NMD mice is specific to certain regions.

KDM6B was primarily expressed in ACC neurons

To determine the distribution of KDM6B in the ACC, we performed immunofluorescence staining on brain coronal sections from CON mice and NMD mice (Figure 3(a)). The results revealed a significantly higher percentage of KDM6B positive cells in the ACC of NMD mice compared to CON mice (Figure 3(b), n = 4, $^{***}p < .001$, two sample t test). Quantitative analysis showed that the percentage of KDM6B localization with NeuN (a marker of neurons), GFAP (a marker of astrocytes), and Iba1 (a marker of microglia) was 58.87 %, 3.52 %, and 3.74 % in CON mice, and 65.95 %, 3.24 %, and 1.94 % in NMD mice. KDM6B was predominately co-localized with NeuN, and only a small number of KDM6B was co-labeled with GFAP and Iba1 in ACC of CON and NMD mice (Figure 3(c), n = 4, $^{*}p < .05$, two sample t test).

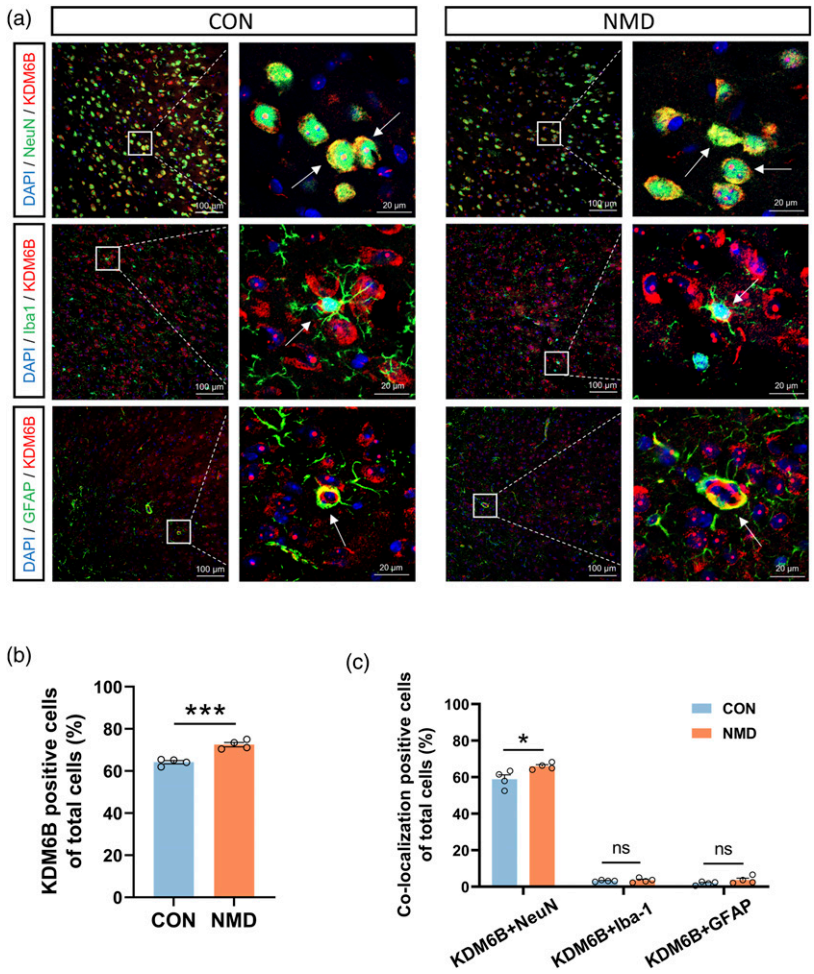

Figure 3. KDM6B was predominantly expressed in neurons in the ACC, and NMD increased KDM6B-positive neurons in the ACC. (a) Representative immunofluorescence images of KDM6B with NeuN, Iba1, and GFAP (Bar = 100 μm). The enlarged pictures in the right panel were to show the co-localization of KDM6B (red) with NeuN (green), Iba1 (green), and GFAP (green) (Bar = 20 μm). The yellow staining indicates co-localization. (b) Analysis of KDM6B positive cells in the ACC of CON and NMD mice ($n = 4$, $^{***}p < .001$, two sample t test). (c) Analysis of co-localization ratio of KDM6B with NeuN, Iba1, and GFAP ($n = 4$, $^{*}p < .05$, two sample t test).

Injection of GSK-J4 in ACC alleviated chronic visceral pain and upregulated H3K27me3 expression in NMD mice

To investigate the role of KDM6B in the regulation of chronic visceral pain in NMD mice, GSK-J4 was injected into the ACC (Figure 4(a)). Following a single injection of GSK-J4, there was no change in the CRD threshold injected with 0.005 mg/kg GSK-J4. However, the CRD threshold injected with 0.025 mg/kg GSK-J4 and 0.1 mg/kg GSK-J4 were significantly elevated 1-4 h post-injection compared to mice injected with DMSO (Figure 4(b), $n = 5$, $^{***}p < .001$, $^{\#\#\#}p < .001$, two-way ANOVA followed by Bonferroni's test). Considering the toxicity and potency of GSK-J4, we used 0.025 mg/kg for 5 consecutive days of injection and found that the CRD threshold in NMD mice were significantly elevated 1-6 h after the last injection, without affecting CON mice (Figure 4(c), $n = 6$ per group, $^{***}p < .001$, two-way ANOVA followed by Bonferroni's test). Subsequently, western blotting showed that the H3K27me3 expression was upregulated (Figure 4(d) and (e), $n = 6$, $^{*}p < .05$, two sample t test) in the ACC of NMD mice after GSK-J4 injection. These data suggest that injection of GSK-J4 into the ACC upregulated H3K27me3 expression and alleviated chronic visceral pain of NMD mice.

Injection of GSK-J4 in ACC alleviated anxiety-like behaviors in NMD mice

To investigate the role of KDM6B in the regulation of anxiety-like behaviors in NMD and CON mice. NMD and CON mice injected with 0.025 mg/kg GSK-J4 were subjected to the open field test, elevated zero maze test, and rotarod test. In the open field test, the results indicate that GSK-J4 mice in the NMD group spent significantly more time in the center zone and less time in the corner zone compared with the DMSO mice, without affecting

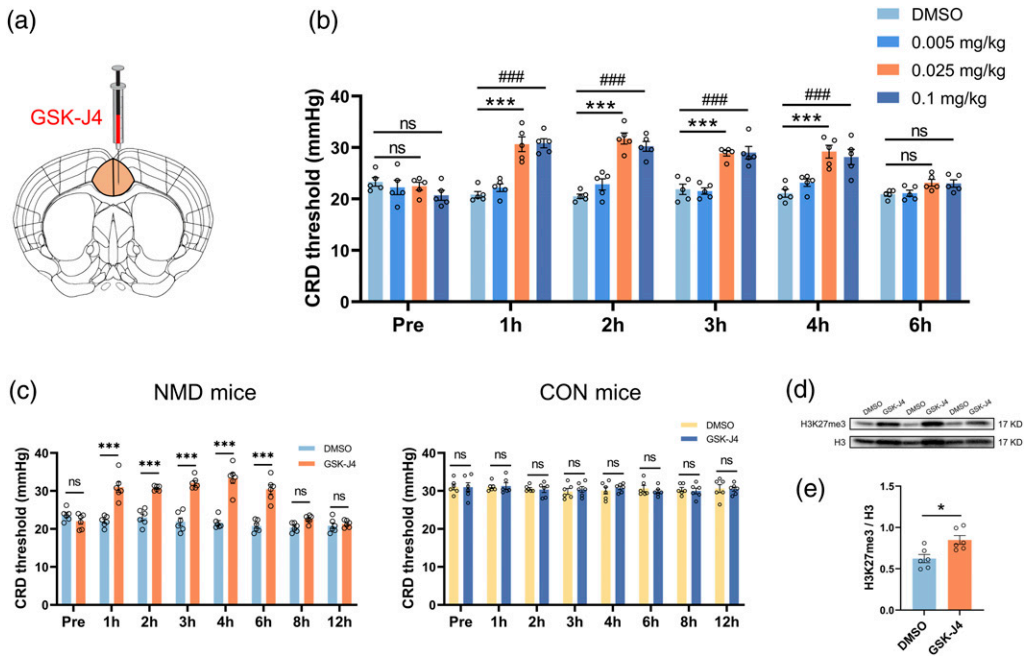

Figure 4. Injection of GSK-J4 in the ACC alleviated chronic visceral pain in NMD mice. (a) Schematic diagram of injecting GSK-J4 into the ACC of NMD mice. (b) CRD threshold of NMD mice at different time points after single injections of DMSO and different concentrations (0.005 mg/kg, 0.025 mg/kg, 0.1 mg/kg) of GSK-J4 ($n = 5$, $^{***}p < .001$, $^{\#\#\#}p < .001$, * Indicates the significance of group 0.025 mg/kg compared to group DMSO, # Indicates the significance of group 0.1 mg/kg compared to group DMSO, two-way ANOVA followed by Bonferroni's test). (c) CRD threshold of NMD and CON mice at different time points after receiving an injection of 0.025 mg/kg GSK-J4 for 5 days ($n = 6$, $^{***}p < .001$, two-way ANOVA followed by Bonferroni's test). (d) Representative western blotting of H3K27me3 and H3 in the ACC of DMSO and GSK-J4 mice. (e) Quantification of H3K27me3 expression level in the ACC of DMSO and GSK-J4 mice ($n = 6$, $^{*}p < .05$, two sample t test).

CON mice (Figure 5(a)–(c), $n = 6$ per group, $^{**}p < .01$, $^{***}p < .001$, two sample t test). GSK-J4 mice also entered the center zone significantly more than DMSO mice (Figure 5(d), $n = 6$ per group, $^{**}p < .01$, two sample t test), indicating that GSK-J4 mice had more desire to explore. However, GSK-J4 injection had no effect on active time and total distance in the open field in NMD and CON mice (Figure 5(e)–(f), $n = 6$ per group, two sample t test). In the elevated zero maze, GSK-J4 mice in the NMD group spent significantly more time exploring open zone compared to DMSO mice, without altering CON mice (Figure 5(g)–(h), $n = 6$ per group, $^{*}p < .05$, two sample t test). However, injection of GSK-J4 unaffected the distance traveled and the number of entries into the open area in NMD and CON mice (Figure 5(i)–(j), $n = 6$ per group, two sample t test). Furthermore, the data of the rotarod test showed unaltered the latency to fall of NMD and CON mice (Figure 5(k), $n = 6$ per group, Mann Whitney test). These results suggest that injection of GSK-J4 into the ACC alleviated anxiety-like behaviors in NMD mice, while unaffecting CON mice.

KDM6B upregulated NR2B expression by demethylating H3K27me3 in the NR2B promoter region in ACC

To determine the mechanism by which KDM6B regulates chronic visceral pain in NMD mice, the ChIP sequencing database was consulted and identified NR2B may be a potential target for KDM6B. We employed qPCR and western blotting to assess the expression of NR2B mRNA and protein expression in CON, NMD, DMSO, and GSK-J4 four groups. Our findings revealed a significantly elevated expression of NR2B mRNA (Figure 6(a), $n = 3$, $^{**}p < .01$, two sample t test) and protein (Figure 6(b) and (c), $n = 6$, $^{*}p < .05$, two sample t test) in NMD mice compared to CON mice. However, administration of GSK-J4 resulted in a significant reduction in NR2B mRNA (Figure 6(d), $n = 3$, $^{*}p < .05$, two sample t test) and protein (Figure 6(e) and (f), $n = 6$, $^{**}p < .01$, Mann Whitney test) expression among NMD mice. The interaction mechanism between KDM6B and NR2B was further investigated through ChIP analysis. The NR2B promoter region, located 2000 bp upstream of the transcription start site of the NR2B gene, was selected for analysis (Figure 6(g)). The same samples were used to detect four primers by PCR, and P2 was found to have the best amplification effect (Figure 6(h)). ChIP was performed to extract DNA fragments bound to H3K27me3 in ACC from CON, NMD, DMSO, and GSK-J4 groups. Subsequently, these four samples were subjected to PCR (Figure 6(i)) and qPCR analyses using the P2 primer. The results showed that the NR2B promoter binding to H3K27me3 in ACC of NMD mice was significantly lower than that of CON mice (Figure 6(j), $n = 4$, $^{**}p < .01$, two sample t test). Compared

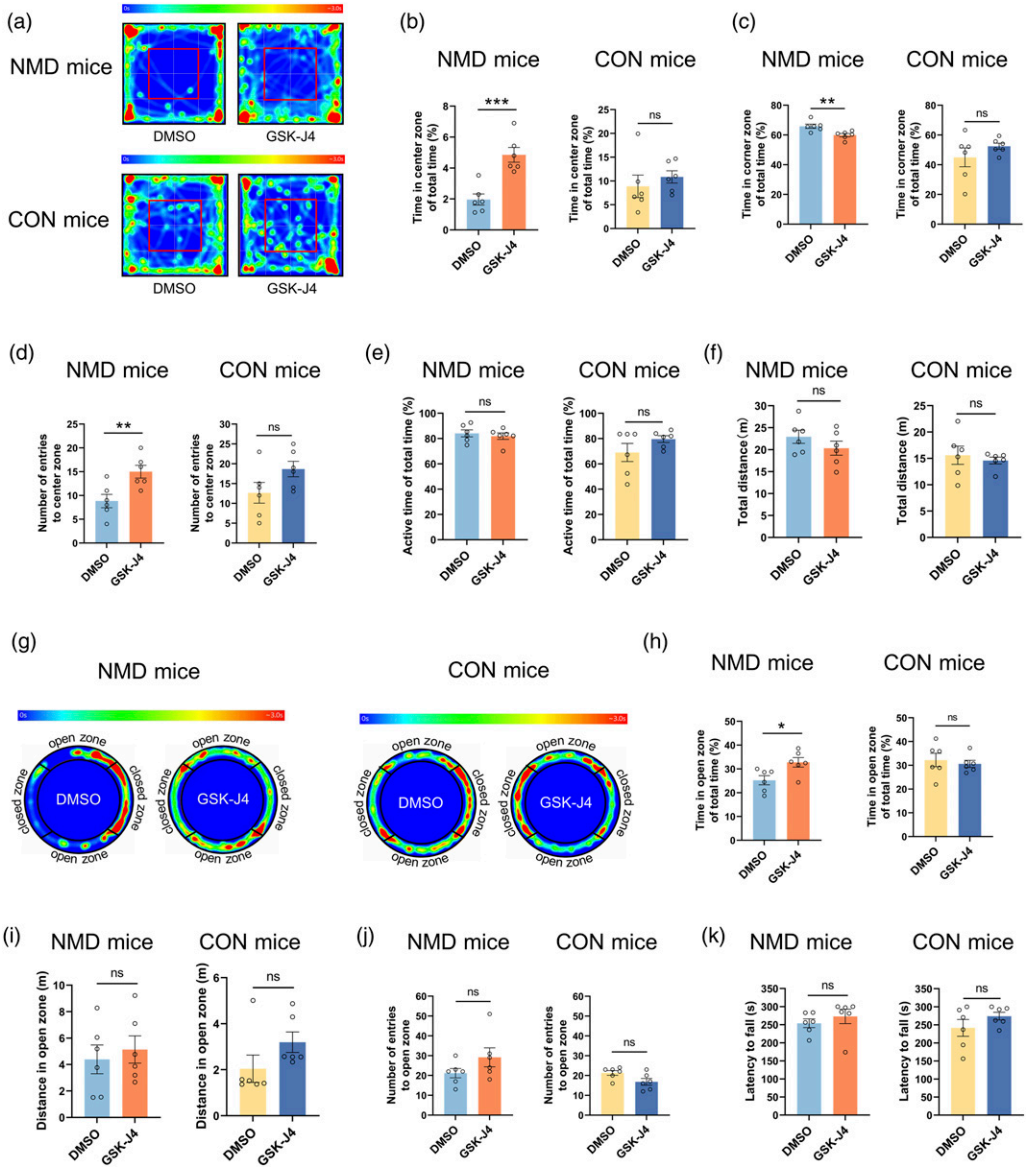

Figure 5. Injection of GSK-J4 in the ACC alleviated anxiety-like behaviors in NMD mice. (a) Heat maps of NMD and CON mice injected with DMSO and GSK-J4 in the 5 min open field tests were detected by ANY-maze (the red square represents the center zone). (b)-(f) Analysis of time in center zone of total time (b), time in corner zone of total time (c), number of entries to center zone (d), active time of total time (e), total distance (f) of NMD and CON mice injected with DMSO and GSK-J4 in the open field test ($n = 6$, $^{**}p < .01$, $^{***}p < .001$, two sample t test). (g) Heat maps of NMD and CON mice injected with DMSO and GSK-J4 in the 3 min elevated zero maze tests were detected by ANY-maze. (h)-(j) Analysis of time in open zone of total time (h), distance in open zone (i), number of entries to open zone (j) of NMD and CON mice injected with DMSO and GSK-J4 in the elevated zero maze test ($n = 6$, $^{*}p < .05$, two sample t test). (k) Analysis of latency to fall of NMD and CON mice injected with DMSO and GSK-J4 in the rotarod test ($n = 6$, Mann Whitney test).

with DMSO-injected NMD mice, NMD mice injected with GSK-J4 had significantly increased NR2B promoters that bind to H3K27me3 in ACC (Figure 6(k), $n = 4$, $^{**}p < .01$, two sample t test). These results suggest that upregulation of KDM6B protein levels in ACC led to a decrease in H3K27me3 bound to the NR2B promoter region, thereby increasing NR2B transcription. This process might contribute to chronic visceral pain and anxiety-like behaviors in NMD mice.

Discussion

Irritable bowel syndrome (IBS) stands as one of the most common gastrointestinal issues faced by physicians.[55] Currently, there is a lack of clear and effective treatments for IBS.[56] Elucidating the underlying molecular mechanisms of central sensitization of chronic visceral pain in patients with IBS is a considerable challenge and a critical process in the development of clinical therapies. In the present study, we

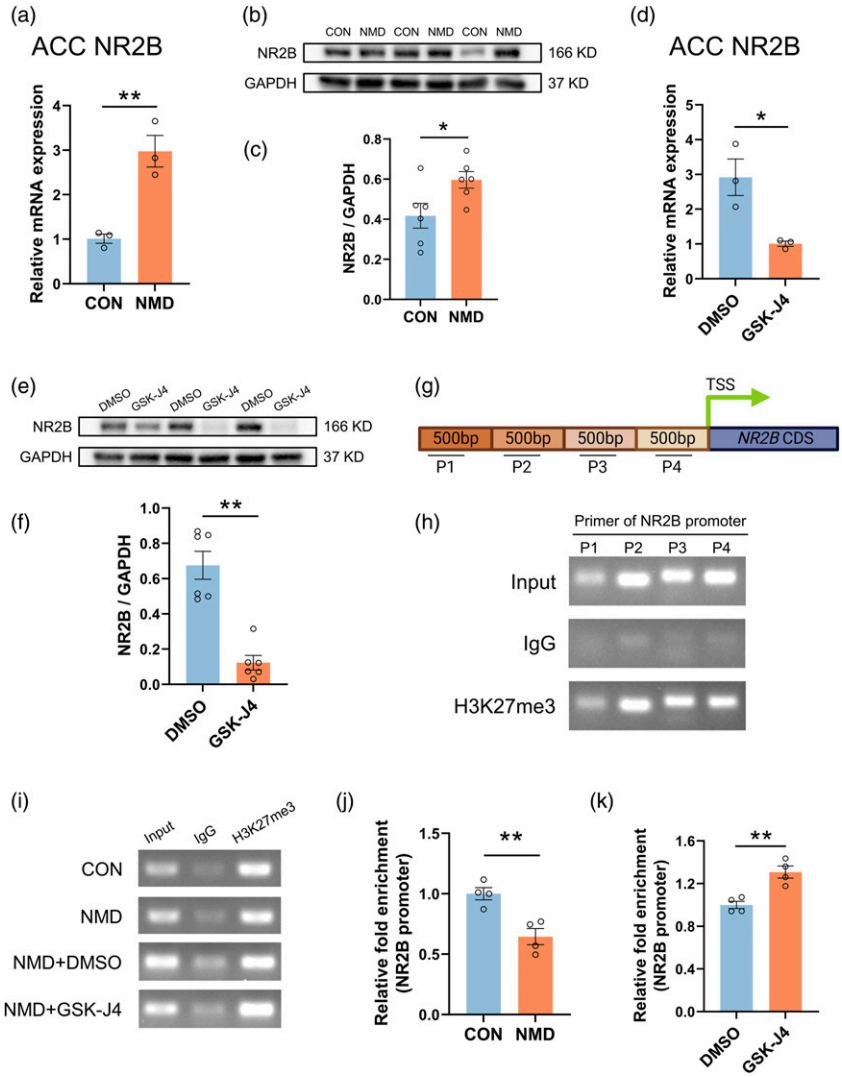

Figure 6. KDM6B increased the expression of NR2B by promoting H3K27me3 demethylation in the NR2B promoter region in ACC, which was reversed by GSK-J4. (a) Quantification of NR2B mRNA expression in the ACC of CON and NMD mice ($n = 3$, $^{**}p < .01$, two sample t test). (b) Representative western blotting of NR2B, GAPDH in the ACC of CON and NMD mice. (c) Quantification of NR2B expression level in the ACC of CON and NMD mice ($n = 6$, $^{*}p < .05$, two sample t test). (d) Quantification of NR2B mRNA expression in the ACC of DMSO and GSK-J4 mice ($n = 3$, $^{*}p < .05$, two sample t test). (e) Representative western blotting of NR2B, GAPDH in the ACC of DMSO and GSK-J4 mice. (f) Quantification of NR2B expression level in the ACC of DMSO and GSK-J4 mice ($n = 6$, $^{**}p < .01$, Mann Whitney test). (g) Four primer pairs were designed by selecting DNA fragments from the NR2B promoter region. (h) Representative PCR image showed the products amplified by all primers (P1 to P4) for the NR2B promoter gene when DNA fragments of input, IgG, and H3K27me3 were used. (i) Representative PCR image showed the products amplified by P2 primer using input, IgG, and H3K27me3 samples from CON, NMD, DMSO, and GSK-J4 mice. (j) Quantification of relative fold enrichment in the ACC of CON and NMD mice ($n = 4$, $^{**}p < .01$, two sample t test). (k) Quantification of relative fold enrichment in the ACC of DMSO and GSK-J4 mice ($n = 4$, $^{**}p < .01$, two sample t test).

offer robust evidence highlighting the critical role of KDM6B in the processing of chronic visceral pain. Increasing evidence supports the role of epigenetics in modulating the development of chronic visceral pain. Previous studies have found demethylation of the *p2x7r* gene in the spinal cord of neonatal colonic inflammation (NCI) rats, contributing to the development of chronic visceral pain.[42] Similar findings were observed in the brain, where the stress model rats showed a significant reduction in H3K9 acetylation at the glucocorticoid receptor (GR) promoter in the amygdala.[57,58] These studies indicated that epigenetics plays a significant role in chronic visceral pain. However, this has not been reported to occur in the cerebral cortex. Our study identifies for the first time an epigenetic regulatory event in the ACC in chronic visceral pain, which is the demethylation of H3K27me3 mediated by KDM6B. Our data reveals that inhibiting KDM6B with GSK-J4 in the ACC of NMD mice elevated H3K27me3 expression and alleviated chronic

visceral pain. This demonstrates that KDM6B-mediated H3K27me3 demethylation is essential for the development of chronic visceral pain. This result is supported by previous study in which H3K27me3 expression was significantly increased in the cerebral cortex after systemic injection of cannabidiol in rats.[59] In addition, drugs were injected only into the unilateral ACC in this study. Previous studies have shown that unilateral ACC injection of drugs can relieve chronic visceral pain and cause less harm to animals.[29,60] This was confirmed by our results.

Notably, we found that KDM6B expression was specifically upregulated in the ACC, which was not observed in PFC and IC. This suggests that ACC may have a possible specific role in chronic visceral pain and anxiety-like behaviors comorbidities and may be a potentially critical target for treatment. Similar results have been found in previous studies, where ACC plays an important role in the development of chronic visceral pain and anxiety-like behaviors.[34,61] Crucially, our findings indicate that KDM6B plays a regulatory role in the expression of NR2B, a crucial subunit of the NMDA receptor involved in processes such as learning, pain perception, and emotion processing.[62] In this study, we demonstrate that KDM6B reduces the enrichment of H3K27me3 in the NR2B promoter region in the ACC of NMD mice, resulting in increased NR2B expression, which was reversed after injection of GSK-J4. This suggests that NR2B acts as a downstream of KDM6B, perhaps underpinning its role in regulating chronic visceral pain. Although in the present study we did not inhibit NR2B and assess its effect on chronic visceral pain, previous studies have demonstrated this.[33,63] In addition, our results are supported by a previous study that shown increased enrichment of H3K27me3 at the NR2B promoter region in the prefrontal cortex of schizophrenia (SCZ) rats.[64]

It is important to note that we only included male mice in this study, due to the fact that the physiological cycle of female mice and their estrogen affects the assessment of visceral pain behavior, which in turn perhaps leads to inaccurate data.[65,66] We will include female mice in future studies to obtain more generalized results.

In summary, our study demonstrates that KDM6B mediates the demethylation of H3K27me3 within the ACC, thereby regulating the expression of NR2B involved in the development of chronic visceral pain and anxiety-like behaviors. These findings unveil a novel pathway of ACC in the regulation of chronic visceral pain, offering a potential new target for the treatment of IBS patients suffering from chronic visceral pain.

Author contributions

Z-L.Y and J-N.L performed experiments and analyzed data. J-J.Z and T-T.H prepared figures and the manuscript. Y-R.X and Z-W.H analyzed data and prepared figures. Y-C.L analyzed data and revised the manuscript. G-Y.X designed experiments, supervised the experiments, and finalized the manuscript. All the authors have read and approved the paper.

Declaration of conflicting interests

The author(s) declared no potential conflicts of interest with respect to the research, authorship, and/or publication of this article.

Funding

The author(s) disclosed receipt of the following financial support for the research, authorship, and/or publication of this article: This work was supported by grants from National Natural Science Foundation of China (81920108016 and 32230041) and Postdoctoral Fellowship Program of CPSF under Grant Number GZC20231890.

ORCID iDs

Jin-Nan Lu https://orcid.org/0009-0003-8138-5124
Guang-Yin Xu https://orcid.org/0000-0002-5495-4120

References

1. Grundy L, Erickson A, Brierley SM. Visceral pain. *Annu Rev Physiol* 2019; 81: 261–284. DOI: 10.1146/annurev-physiol-020518-114525.
2. Gebhart GF, Bielefeldt K. Physiology of visceral pain. *Compr Physiol* 2016; 6: 1609–1633. DOI: 10.1002/cphy.c150049.
3. Weng RX, Wei YX, Li YC, Xu X, Zhuang JB, Xu GY, Li R. Folic acid attenuates chronic visceral pain by reducing clostridiales abundance and hydrogen sulfide production. *Mol Pain* 2023; 19: 17448069221149834. DOI: 10.1177/17448069221149834.
4. Brierley SM, Grundy L, Castro J, Harrington AM, Hannig G, Camilleri M. Guanylate cyclase-C agonists as peripherally acting treatments of chronic visceral pain. *Trends in pharmacological sciences* 2022; 43: 110–122. DOI: 10.1016/j.tips.2021.11.002.
5. Enck P, Aziz Q, Barbara G, Farmer AD, Fukudo S, Mayer EA, Niesler B, Quigley EM, Rajilić-Stojanović M, Schemann M, Schwille-Kiuntke J, Simren M, Zipfel S, Spiller RC. Irritable bowel syndrome. *Nat Rev Dis Prim* 2016; 2: 16014. DOI: 10.1038/nrdp.2016.14.
6. Mayer EA, Ryu HJ, Bhatt RR. The neurobiology of irritable bowel syndrome. *Mol Psychiatry* 2023; 28: 1451–1465. DOI: 10.1038/s41380-023-01972-w.
7. Ford AC, Lacy BE, Talley NJ. Irritable bowel syndrome. *N Engl J Med* 2017; 376: 2566–2578. DOI: 10.1056/NEJMra1607547.
8. Ford AC, Sperber AD, Corsetti M, Camilleri M. Irritable bowel syndrome. *Lancet* 2020; 396: 1675–1688. DOI: 10.1016/s0140-6736(20)31548-8.
9. Camilleri M, Boeckxstaens G. Irritable bowel syndrome: treatment based on pathophysiology and biomarkers. *Gut* 2023; 72: 590–599. DOI: 10.1136/gutjnl-2022-328515.
10. Chey WD, Kurlander J, Eswaran S. Irritable bowel syndrome: a clinical review. *JAMA* 2015; 313: 949–958. DOI: 10.1001/jama.2015.0954.

11. Sood R, Law GR, Ford AC. Diagnosis of IBS: symptoms, symptom-based criteria, biomarkers or 'psychomarkers'? *Nat Rev Gastroenterol Hepatol* 2014; 11: 683–691. DOI: 10.1038/nrgastro.2014.127.
12. Lv MD, Wei YX, Chen JP, Cao MY, Wang QL, Hu S. Melatonin attenuated chronic visceral pain by reducing Na(v)1.8 expression and nociceptive neuronal sensitization. *Mol Pain* 2023; 19: 17448069231170072. DOI: 10.1177/17448069231170072.
13. Ghoshal UC, Gwee KA. Post-infectious IBS, tropical sprue and small intestinal bacterial overgrowth: the missing link. *Nat Rev Gastroenterol Hepatol* 2017; 14: 435–441. DOI: 10.1038/nrgastro.2017.37.
14. Sun Q, Weng RX, Li JH, Li YC, Xu JT, Li R, Lu X, Xu GY. Rab27a-mediated exosome secretion in anterior cingulate cortex contributes to colorectal visceral pain in adult mice with neonatal maternal deprivation. *Am J Physiol Gastrointest Liver Physiol* 2023; 325: G356–g367. DOI: 10.1152/ajpgi.00029.2023.
15. Wu K, Gao JH, Hua R, Peng XH, Wang H, Zhang YM. Predisposition of neonatal maternal separation to visceral hypersensitivity via downregulation of small-conductance calcium-activated potassium channel subtype 2 (SK2) in mice. *Neural Plast* 2020; 2020: 8876230. DOI: 10.1155/2020/8876230.
16. Journée SH, Mathis VP, Fillinger C, Veinante P, Yalcin I. Janus effect of the anterior cingulate cortex: pain and emotion. *Neurosci Biobehav Rev* 2023; 153: 105362. DOI: 10.1016/j.neubiorev.2023.105362.
17. Zhang TT, Guo SS, Wang HY, Jing Q, Yi X, Hu ZH, Yu XR, Xu TL, Liu MG, Zhao X. An anterior cingulate cortex-to-midbrain projection controls chronic itch in mice. *Neurosci Bull* 2023; 39: 793–807. DOI: 10.1007/s12264-022-00996-6.
18. Xiao X, Ding M, Zhang YQ. Role of the anterior cingulate cortex in translational pain research. *Neurosci Bull* 2021; 37: 405–422. DOI: 10.1007/s12264-020-00615-2.
19. Becker LJ, Fillinger C, Waegaert R, Journée SH, Hener P, Ayazgok B, Humo M, Karatas M, Thouaye M, Gaikwad M, Degiorgis L, Santin MDN, Mondino M, Barrot M, Ibrahim EC, Turecki G, Belzeaux R, Veinante P, Harsan LA, Hugel S, Lutz PE, Yalcin I. The basolateral amygdala-anterior cingulate pathway contributes to depression-like behaviors and comorbidity with chronic pain behaviors in male mice. *Nat Commun* 2023; 14: 2198. DOI: 10.1038/s41467-023-37878-y.
20. Barthas F, Sellmeijer J, Hugel S, Waltisperger E, Barrot M, Yalcin I. The anterior cingulate cortex is a critical hub for pain-induced depression. *Biol Psychiatr* 2015; 77: 236–245. DOI: 10.1016/j.biopsych.2014.08.004.
21. Li ZZ, Han WJ, Sun ZC, Chen Y, Sun JY, Cai GH, Liu WN, Wang TZ, Xie YD, Mao HH, Wang F, Ma SB, Wang FD, Xie RG, Wu SX, Luo C. Extracellular matrix protein laminin β1 regulates pain sensitivity and anxiodepression-like behaviors in mice. *J Clin Invest* 2021; 131. DOI: 10.1172/jci146323.
22. Bliss TV, Collingridge GL, Kaang BK, Zhuo M. Synaptic plasticity in the anterior cingulate cortex in acute and chronic pain. *Nat Rev Neurosci* 2016; 17: 485–496. DOI: 10.1038/nrn.2016.68.
23. Ru Q, Lu Y, Saifullah AB, Blanco FA, Yao C, Cata JP, Li DP, Tolias KF, Li L. TIAM1-mediated synaptic plasticity underlies comorbid depression-like and ketamine antidepressant-like actions in chronic pain. *J Clin Invest* 2022; 132. DOI: 10.1172/jci158545.
24. Yoshino A, Okamoto Y, Onoda K, Yoshimura S, Kunisato Y, Demoto Y, Okada G, Yamawaki S. Sadness enhances the experience of pain via neural activation in the anterior cingulate cortex and amygdala: an fMRI study. *Neuroimage* 2010; 50: 1194–1201. DOI: 10.1016/j.neuroimage.2009.11.079.
25. Dong Z, Zhan T, Sun H, Wang J, Duan G, Zhang Y, Chen Y, Huang Y, Xu S. Astrocytic ERK/STAT1 signaling contributes to maintenance of stress-related visceral hypersensitivity in rats. *J Pain* 2022; 23: 1973–1988. DOI: 10.1016/j.jpain.2022.07.006.
26. Moloney RD, Sajjad J, Foley T, Felice VD, Dinan TG, Cryan JF, O'Mahony SM. Estrous cycle influences excitatory amino acid transport and visceral pain sensitivity in the rat: effects of early-life stress. *Biol Sex Differ* 2016; 7: 33. DOI: 10.1186/s13293-016-0086-6.
27. Cao Z, Wu X, Chen S, Fan J, Zhang R, Owyang C, Li Y. Anterior cingulate cortex modulates visceral pain as measured by visceromotor responses in viscerally hypersensitive rats. *Gastroenterology* 2008; 134: 535–543. DOI: 10.1053/j.gastro.2007.11.057.
28. Liu SB, Wang XS, Yue J, Yang L, Li XH, Hu LN, Lu JS, Song Q, Zhang K, Yang Q, Zhang MM, Bernabucci M, Zhao MG, Zhuo M. Cyclic AMP-dependent positive feedback signaling pathways in the cortex contributes to visceral pain. *J Neurochem* 2020; 153: 252–263. DOI: 10.1111/jnc.14903.
29. Tian YQ, Li JH, Li YC, Xu YC, Zhang PA, Wang Q, Li R, Xu GY. Overexpression of GRK6 alleviates chronic visceral hypersensitivity through downregulation of P2Y6 receptors in anterior cingulate cortex of rats with prenatal maternal stress. *CNS Neurosci Ther* 2022; 28: 851–861. DOI: 10.1111/cns.13827.
30. Cao B, Wang J, Mu L, Poon DC, Li Y. Impairment of decision making associated with disruption of phase-locking in the anterior cingulate cortex in viscerally hypersensitive rats. *Exp Neurol* 2016; 286: 21–31. DOI: 10.1016/j.expneurol.2016.09.010.
31. Liu SB, Zhang MM, Cheng LF, Shi J, Lu JS, Zhuo M. Long-term upregulation of cortical glutamatergic AMPA receptors in a mouse model of chronic visceral pain. *Mol Brain* 2015; 8: 76. DOI: 10.1186/s13041-015-0169-z.
32. Wang XS, Yue J, Hu LN, Tian Z, Yang LK, Lu L, Zhao MG, Liu SB. Effects of CPEB1 in the anterior cingulate cortex on visceral pain in mice. *Brain Res* 2019; 1712: 55–62. DOI: 10.1016/j.brainres.2019.02.001.
33. Xu QY, Zhang HL, Du H, Li YC, Ji FH, Li R, Xu GY. Identification of a glutamatergic claustrum-anterior cingulate cortex circuit for visceral pain processing. *J Neurosci : The Official Journal of the Society for Neuroscience* 2022; 42: 8154–8168. DOI: 10.1523/jneurosci.0779-22.2022.

34. Wu K, Liu YY, Shao S, Song W, Chen XH, Dong YT, Zhang YM. The microglial innate immune receptors TREM-1 and TREM-2 in the anterior cingulate cortex (ACC) drive visceral hypersensitivity and depressive-like behaviors following DSS-induced colitis. *Brain Behav Immun* 2023; 112: 96–117. DOI: 10.1016/j.bbi.2023.06.003.
35. Bai G, Ren K, Dubner R. Epigenetic regulation of persistent pain. *Transl Res: The Journal of Laboratory and Clinical Medicine* 2015; 165: 177–199. DOI: 10.1016/j.trsl.2014.05.012.
36. Odell DW. Epigenetics of pain mediators. *Curr Opin Anaesthesiol* 2018; 31: 402–406. DOI: 10.1097/aco.0000000000000613.
37. Liu S, Hagiwara SI, Bhargava A. Early-life adversity, epigenetics, and visceral hypersensitivity. *Neuro Gastroenterol Motil* 2017; 29. DOI: 10.1111/nmo.13170.
38. Hong S, Zheng G, Wiley JW. Epigenetic regulation of genes that modulate chronic stress-induced visceral pain in the peripheral nervous system. *Gastroenterology* 2015; 148: 148–157. DOI: 10.1053/j.gastro.2014.09.032.
39. Wiley JW, Zong Y, Zheng G, Zhu S, Hong S. Histone H3K9 methylation regulates chronic stress and IL-6-induced colon epithelial permeability and visceral pain. *Neuro Gastroenterol Motil* 2020; 32: e13941. DOI: 10.1111/nmo.13941.
40. Tran L, Chaloner A, Sawalha AH, Greenwood Van-Meerveld B. Importance of epigenetic mechanisms in visceral pain induced by chronic water avoidance stress. *Psychoneuroendocrinology* 2013; 38: 898–906. DOI: 10.1016/j.psyneuen.2012.09.016.
41. Louwies T, Greenwood-Van Meerveld B. Sex differences in the epigenetic regulation of chronic visceral pain following unpredictable early life stress. *Neuro Gastroenterol Motil* 2020; 32: e13751. DOI: 10.1111/nmo.13751.
42. Wu YY, Zhang HL, Lu X, Du H, Li YC, Zhang PA, Xu GY. Targeting GATA1 and p2x7r locus binding in spinal astrocytes suppresses chronic visceral pain by promoting DNA demethylation. *Neurosci Bull* 2022; 38: 359–372. DOI: 10.1007/s12264-021-00799-1.
43. Swahari V, West AE. Histone demethylases in neuronal differentiation, plasticity, and disease. *Curr Opin Neurobiol* 2019; 59: 9–15. DOI: 10.1016/j.conb.2019.02.009.
44. Ding Y, Yao Y, Gong X, Zhuo Q, Chen J, Tian M, Farzaneh M. JMJD3: a critical epigenetic regulator in stem cell fate. *Cell Commun Signal : CCS* 2021; 19: 72. DOI: 10.1186/s12964-021-00753-8.
45. Zhang X, Liu L, Yuan X, Wei Y, Wei X. JMJD3 in the regulation of human diseases. *Protein & cell* 2019; 10: 864–882. DOI: 10.1007/s13238-019-0653-9.
46. Katsuda Y, Tanaka K, Mori T, Narita M, Takeshima H, Kondo T, Yamabe Y, Matsufuji M, Sato D, Hamada Y, Yamaguchi K, Ushijima T, Inada E, Kuzumaki N, Iseki M, Narita M. Histone modification of pain-related gene expression in spinal cord neurons under a persistent postsurgical pain-like state by electrocautery. *Mol Brain* 2021; 14: 146. DOI: 10.1186/s13041-021-00854-y.
47. Lee J, Choi H, Park C, Jeon S, Yune T. Jmjd3 mediates neuropathic pain by inducing macrophage infiltration and activation in lumbar spinal stenosis animal model. *Int J Mol Sci* 2021; 22: 2021. DOI: 10.3390/ijms222413426.
48. Li L, Bai L, Yang K, Zhang J, Gao Y, Jiang M, Yang Y, Zhang X, Wang L, Wang X, Qiao Y, Xu JT. KDM6B epigenetically regulated-interleukin-6 expression in the dorsal root ganglia and spinal dorsal horn contributes to the development and maintenance of neuropathic pain following peripheral nerve injury in male rats. *Brain Behav Immun* 2021; 98: 265–282. DOI: 10.1016/j.bbi.2021.08.231.
49. Qiao Y, Li L, Bai L, Gao Y, Yang Y, Wang L, Wang X, Liang Z, Xu JT. Upregulation of lysine-specific demethylase 6B aggravates inflammatory pain through H3K27me3 demethylation-dependent production of TNF-α in the dorsal root ganglia and spinal dorsal horn in rats. *CNS Neurosci Ther* 2023; 29: 3479–3492. DOI: 10.1111/cns.14281.
50. Barreau F, Ferrier L, Fioramonti J, Bueno L. New insights in the etiology and pathophysiology of irritable bowel syndrome: contribution of neonatal stress models. *Pediatr Res* 2007; 62: 240–245. DOI: 10.1203/PDR.0b013e3180db2949.
51. Hu S, Sun Q, Du WJ, Song J, Li X, Zhang PA, Xu JT, Xu GY. Adult stress promotes purinergic signaling to induce visceral pain in rats with neonatal maternal deprivation. *Neurosci Bull* 2020; 36: 1271–1280. DOI: 10.1007/s12264-020-00575-7.
52. Huang ST, Song ZJ, Liu Y, Luo WC, Yin Q, Zhang YM. BNST(AV) (GABA)-PVN(CRF) circuit regulates visceral hypersensitivity induced by maternal separation in vgat-cre mice. *Front Pharmacol* 2021; 12: 615202. DOI: 10.3389/fphar.2021.615202.
53. Zhang FC, Wei YX, Weng RX, Xu QY, Li R, Yu Y, Xu GY. Paraventricular thalamus-insular cortex circuit mediates colorectal visceral pain induced by neonatal colonic inflammation in mice. *CNS Neurosci Ther* 2023. DOI: 10.1111/cns.14534.
54. Yasuda M, Shinoda M, Honda K, Fujita M, Kawata A, Nagashima H, Watanabe M, Shoji N, Takahashi O, Kimoto S, Iwata K. Maternal separation induces orofacial mechanical allodynia in adulthood. *J Dent Res* 2016; 95: 1191–1197. DOI: 10.1177/0022034516661159.
55. Ma C, Congly SE, Novak KL, Belletrutti PJ, Raman M, Woo M, Andrews CN, Nasser Y. Epidemiologic burden and treatment of chronic symptomatic functional bowel disorders in the United States: a nationwide analysis. *Gastroenterology* 2021; 160: 88–98.e84. DOI: 10.1053/j.gastro.2020.09.041.
56. Lazaraki G, Chatzimavroudis G, Katsinelos P. Recent advances in pharmacological treatment of irritable bowel syndrome. *World J Gastroenterol* 2014; 20: 8867–8885. DOI: 10.3748/wjg.v20.i27.8867.
57. Louwies T, Orock A, Greenwood-Van Meerveld B. Stress-induced visceral pain in female rats is associated with epigenetic remodeling in the central nucleus of the amygdala. *Neurobiol Stress* 2021; 15: 100386. DOI: 10.1016/j.ynstr.2021.100386.
58. Louwies T, Ligon CO, Johnson AC, Greenwood-Van Meerveld B. Targeting epigenetic mechanisms for chronic visceral pain: a

valid approach for the development of novel therapeutics. *Neuro Gastroenterol Motil* 2019; 31: e13500. DOI: 10.1111/nmo.13500.

59. Pastrana-Trejo JC, Duarte-Aké F, Us-Camas R, De-la-Peña C, Parker L, Pertwee RG, Murillo-Rodríguez E. Effects on the post-translational modification of H3K4Me3, H3K9ac, H3K9Me2, H3K27Me3, and H3K36Me2 levels in cerebral cortex, hypothalamus and pons of rats after a systemic administration of cannabidiol: a preliminary study. Central nervous system agents in medicinal *Chemistry* 2021; 21: 142–147. DOI: 10.2174/1871524920666200924114524.
60. Xiao Y, Xie L, Xu QY, Chen L, Chen H, Xu GY, Zhang PA. Transcranial direct current stimulation relieves visceral hypersensitivity via normalizing GluN2B expression and neural activity in anterior cingulate cortex. *J Neurophysiol* 2021; 125: 1787–1797. DOI: 10.1152/jn.00025.2021.
61. Kanazawa M, Hongo M, Fukudo S. Visceral hypersensitivity in irritable bowel syndrome. *J Gastroenterol Hepatol* 2011; 26(Suppl 3): 119–121. DOI: 10.1111/j.1440-1746.2011.06640.x.
62. Loftis JM, Janowsky A. The N-methyl-D-aspartate receptor subunit NR2B: localization, functional properties, regulation, and clinical implications. *Pharmacol Therapeut* 2003; 97: 55–85. DOI: 10.1016/s0163-7258(02)00302-9.
63. Tan LH, Li KG, Wu YY, Guo MW, Lan Y, Wang S, Zhu WL, Ren XX. Effect of electroacupuncture at different acupoints on the expression of NMDA receptors in ACC and colon in IBS rats. *Evid Based Complement Alternat Med* 2019; 2019: 4213928. DOI: 10.1155/2019/4213928.
64. Gulchina Y, Xu SJ, Snyder MA, Elefant F, Gao WJ. Epigenetic mechanisms underlying NMDA receptor hypofunction in the prefrontal cortex of juvenile animals in the MAM model for schizophrenia. *J Neurochem* 2017; 143: 320–333. DOI: 10.1111/jnc.14101.
65. Athnaiel O, Cantillo S, Paredes S, Knezevic NN. The role of sex hormones in pain-related conditions. *Int J Mol Sci* 2023; 24. DOI: 10.3390/ijms24031866.
66. Jiang Y, Greenwood-Van Meerveld B, Johnson AC, Travagli RA. Role of estrogen and stress on the brain-gut axis. *Am J Physiol Gastrointest Liver Physiol* 2019; 317: G203–g209. DOI: 10.1152/ajpgi.00144.2019.